

Supporting Information

Realizing reusability of leachate for hydrometallurgical recycling of spent lithium cobalt oxide by dynamically regulating the solubility product

*Tao Hu, Taibai Li, Xuncheng Liu, Zhongjie Wang, Liang Lou, Siqu Jing, Xiaohui Yan, Yige Xiong, Junkai Xiong, Xiang Ge**

Department of Materials and Metallurgy, Guizhou University, Guiyang 550025, Guizhou, China

*Corresponding Author

E-mail: xge@gzu.edu.cn (Xiang Ge)

Keywords: Lithium-ion batteries recycle; Deep eutectic solvent; Precipitant-free strategy; K_{sp} regulation; Leachate reusability

Table of content in the supporting data:

Formula S1-S2: quantification of leaching kinetics parameters.

The main reactions involved in the recovery process.

Table S1. A summary of metal leaching from spent LIBs.

Table S2. Energy and economic analysis of Pyrometallurgy, Hydrometallurgy¹ and this work.

Table S3. A brief comparison between Pyrometallurgy, Hydrometallurgy and this work.

Table S4. Solubility Product Constants at 25°C.

Fig. S1. (a) Digital photos showing that wasted LCO can be collected from the spent electrodes followed by thermal treatment to remove the binder and the conductive additives. (b and c) give the TG-DSC curve of (b) 50% PVDF: 50% acetylene black and (c) the black mass directly collected from the wasted electrode measured under air atmosphere at a heating rate of 5°C min⁻¹. (d and e) show the SEM images (d) and the XRD pattern (e) of the LCO collected after the pre-treatment as shown in (a).

Fig. S2. Effect of different water content on cobalt precipitation

Fig. S3. (a) Effect of adding DIW in the DES on the cobalt separation process and (b) the effects of different solid-liquid ratio.

Fig. S4. (a) The leaching rate under different conditions (60-100°C, 0-240 min). (b and c) show the fitting of the activation energy ($E_a = 21.7$ kJ/mol) in the leaching process.

Fig. S5. (a) SEM images of the precipitated brick-like $\text{CoC}_2\text{O}_4 \cdot 2\text{H}_2\text{O}$ phase (a and b) and the annealed Co_3O_4 (c and d). The annealed Co_3O_4 resembles the morphology of

the $\text{CoC}_2\text{O}_4 \cdot 2\text{H}_2\text{O}$ precursor, while pores were formed due to the topological shrinkage of the lattice; (e) the commercial LCO and (f) the regenerated LCO.

Fig. S6. 5x magnification version of digital photos.

Fig. S7. (a) Digital photos visualizing the lithium element can be extracted by direct cooling. (b) XRD patterns of the precipitated lithium compound recovered at different temperatures.

Fig. S8. SEM images of the precipitated Li compound in the form of oxalic salt.

Fig. S9. Energy and economic analysis of other recycling approaches and this work. (a) Cost, (b) revenue and (c) profit for Pyrometallurgy, Hydrometallurgy and this work. Radar charts with parameters in terms of environment and economy for (d) Pyrometallurgy, (f) Hydrometallurgy and (g) this work.

Fig. S10: Cycle performance of DES (90°C, 3 h). (a) Leaching efficiencies of Li and Co at different cycle numbers and (b) digital photos of DES after multiple cycles.

Fig. S11: (a) The CV and (b) EIS spectrum of the recycled and the commercial LCO samples.

Movie S1: Lithium extraction process by dynamically regulating the solubility product (K_{sp}).

Quantification of leaching kinetics parameters

Formula S1:

Assuming that the proportion of Li in the leached ions remains invariant, the apparent reaction rate equation can be derived as follows:

$$1 - (1 - \eta)^{\frac{1}{3}} = Kt \quad (1)$$

where K denotes the rate constant, t represents the leaching time (min)²⁻⁴. This model is suitable for both diffusion control process and chemical reaction control process.

Formula S2:

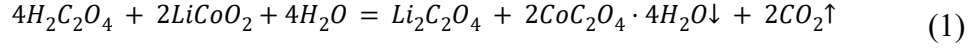
Based on the fitted K at various temperatures, the activation energy E_a can then be calculated using:

$$-\ln K = \frac{E_a}{RT} - \ln A \quad (2)$$

Where A is the pre-exponential factor, R is the molar gas constant, T is the thermodynamic temperature (K), E_a is the apparent activation energy (kJ/mol)^{5,6}.

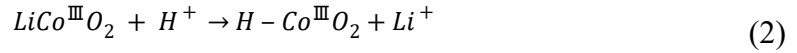
The main reactions involved in the recovery process

Eq.(1) shows the overall leaching process of LCO with ChCl:OA^{4,7}, which results in the separation of Li and Co into different phases (soluble Li⁺ and solid state Co²⁺) as follows:

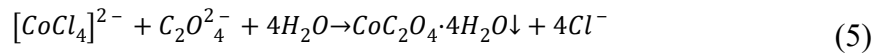
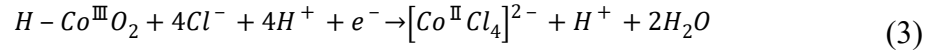


The following equations illustrate the detailed separation mechanism of Li and Co from spent LIBs:

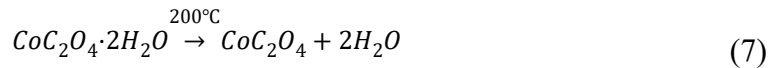
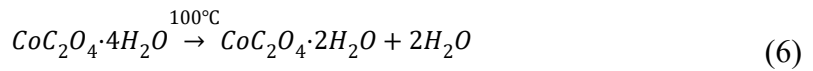
(1) The extraction of Li by DES follows this mechanism⁸:

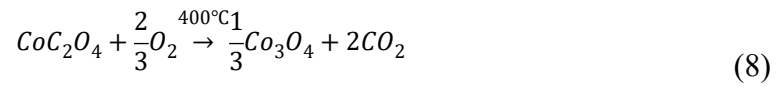


(2) The Co element undergoes the reduction from Co³⁺ to Co²⁺ and forms a chelate complex with C₂O₄²⁻. With the existence deionized water, the cobalt precipitates as a stable compounds of CoC₂O₄•4H₂O as a stable compound⁴. The corresponding reactions are shown in Eqs. (3) - (5).



CoC₂O₄·2H₂O can be obtained by drying at 100°C for 10 h. Afterwards, Co₃O₄ can be prepared by calcination as a precursor for regenerating LCO. The equations involved in this process are described as follows:





The regeneration of LCO material is achieved by using the regenerated Co_3O_4 and $Li_2C_2O_4$ as the precursors with a high temperature solid-phase method. The following equations describe the reactions involved in this process:

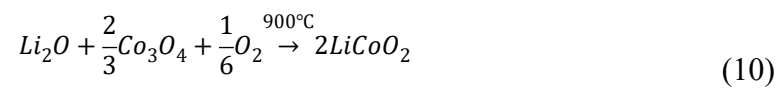


Table S1. A summary of metal leaching from spent LIBs.

Category	Recycling method	Cathode	Condition		Leaching efficiency[%]		Ref.
			Time[min]	Temp[°C]	Li	Co	
Pyrometallurgy	CTR Roasting (Graphite)	LCO	30	1000	98.93	95.72	9
	Salt assisted roasting (H ₂ SO ₄)		120	800	99.3	98.7	10
	Salt assisted roasting ((NH ₄) ₂ SO ₄)		120	400	98	98	11
	Salt assisted roasting ((NH ₄) ₂ SO ₄)		60	400	91.3	93.5	12
Conventional Hydrometallurgy	0.4 M H ₂ SO ₄	LCO	10	200	77	24	13
	0.4 M HNO ₃		10	300	82	37	13
	2 M H ₂ SO ₄ and 0.28 M glucose		240	80	92	88	14
	0.1 M citric acid + 0.02 M ascorbic acid		360	80	100	80	15
	0.1 M iminodiacetic acid+0.02M ascorbic acid		360	80	99	91	16
DESs	ChCl : Malic acid	LCO	240	60	—	81.2	17
	ChCl : Malonic acid		240	60	—	24.4	
	ChCl : EG		1440	180	89.81	50.30	18
	ChCl : EG		1440	160	28.4	23.8	
	ChCl : EG		1440	80		~0	
	ChCl : Urea		1440	160	61.2	64.2	19
	ChCl : Urea		720	170	68.7	89.1	19
	ChCl / Urea		720	180	95	98	19
EG / sulfosalicylic acid		360	110	98	93	20	

	dihydrate						
This work	ChCl / OA	LCO	180	90	~95	~98	

Table S2. Energy and economic analysis of Pyrometallurgy, Hydrometallurgy¹ and this work.

	Pyrometallurgy	Hydrometallurgy	This work
Cost (\$ kg ⁻¹)	4.87	4.35	3.2
Revenue (\$ kg ⁻¹)	4.90	6.35	13.92
Profit (\$ kg ⁻¹)	0.03	2.00	10.72
Energy consumption (MJ kg ⁻¹)	10.71	19.57	5.8
GHG emission (g kg ⁻¹)	2183	1468	449

Table S3. A brief comparison between Pyrometallurgy, Hydrometallurgy and this work.

Pyrometallurgy	Hydrometallurgy	This work
High temperature treatment	Intermediate operation condition	Mild operation condition
High energy consumption	Corrosive acids	Green and energy reservation
With waste disposal	Non-recyclable	Leachant reusable
High GHG emission	Moderate GHG emission	Low GHG emission

Table S4. Solubility Product Constants at 25°C^{7, 21}.

No.	Compound	K _{sp}
1	Co(OH) ₂	1.0 × 10 ⁻¹⁵
2	CoCO ₃	12.0 × 10 ⁻¹¹
3	Ni(OH) ₂	3.1 × 10 ⁻¹⁵
4	NiCO ₃	6.8 × 10 ⁻⁸
5	Mn(OH) ₂	1.7 × 10 ⁻¹³
6	MnCO ₃	3.3 × 10 ⁻¹¹
7	CoC ₂ O ₄	4.09 × 10 ⁻⁸
8	NiC ₂ O ₄	4.31 × 10 ⁻⁹

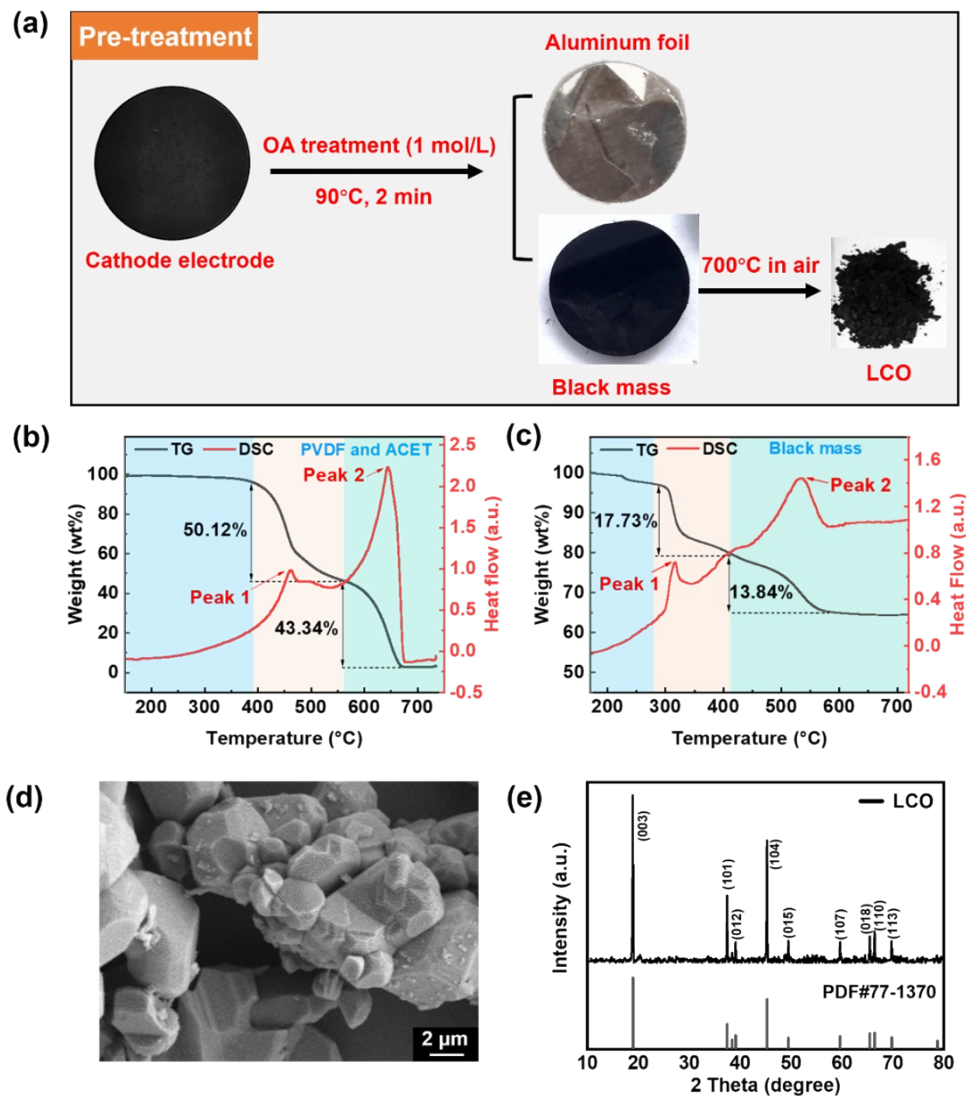


Fig. S1 (a) Digital photos showing that wasted LCO can be collected from the spent electrodes followed by thermal treatment to remove the binder and the conductive additives. (b and c) give the TG-DSC curve of (b) 50% PVDF: 50% acetylene black and (c) the black mass directly collected from the wasted electrode measured under air atmosphere at a heating rate of $5^{\circ}\text{C min}^{-1}$. (d and e) show the SEM images (d) and the XRD pattern (e) of the LCO collected after the pre-treatment as shown in (a).

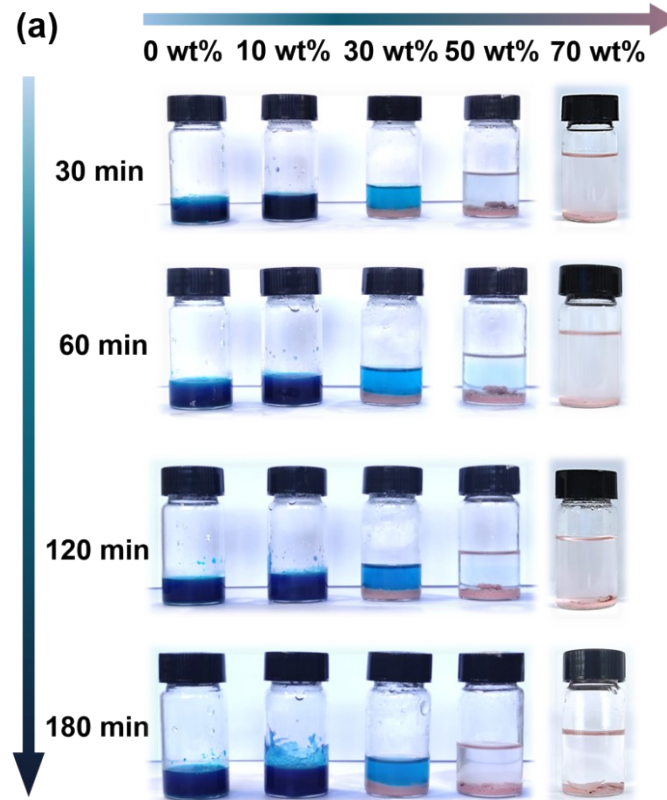


Fig. S2 Effect of different water content on cobalt precipitation

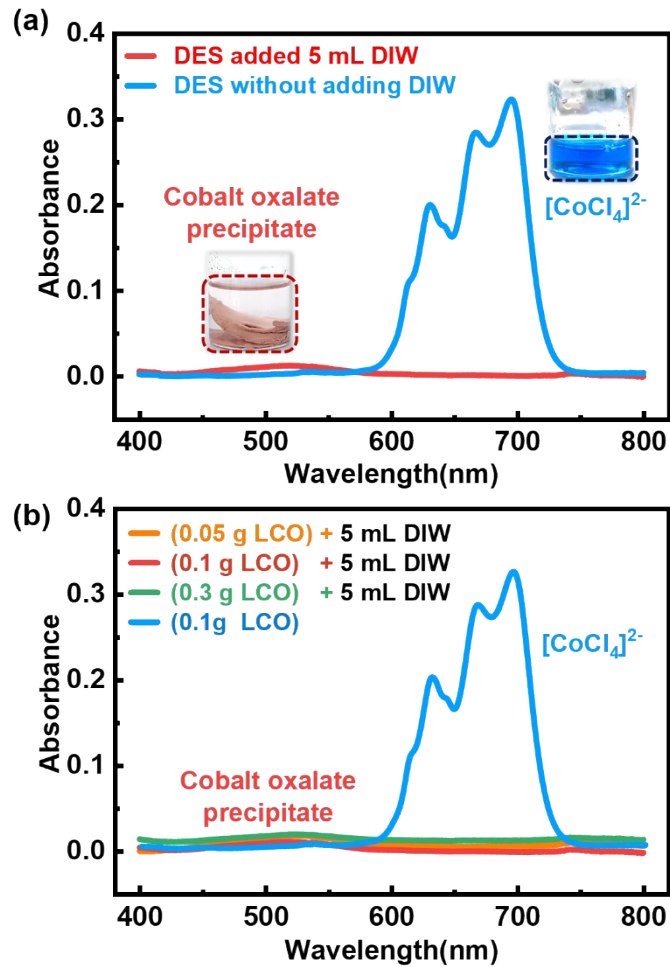


Fig. S3 (a) Effect of adding DIW in the DES on the cobalt separation process and (b) the effects of different solid-liquid ratio. With the existence of DIW, the characteristic peak of $[\text{CoCl}_4]^{2-}$ was not observed in the UV-Vis spectra. For the leaching solution without DIW, three characteristic bands (630, 667 and 696 nm) indicate the formation of $[\text{CoCl}_4]^{2-}$. The results shed light on the transformation process of the cobalt element.

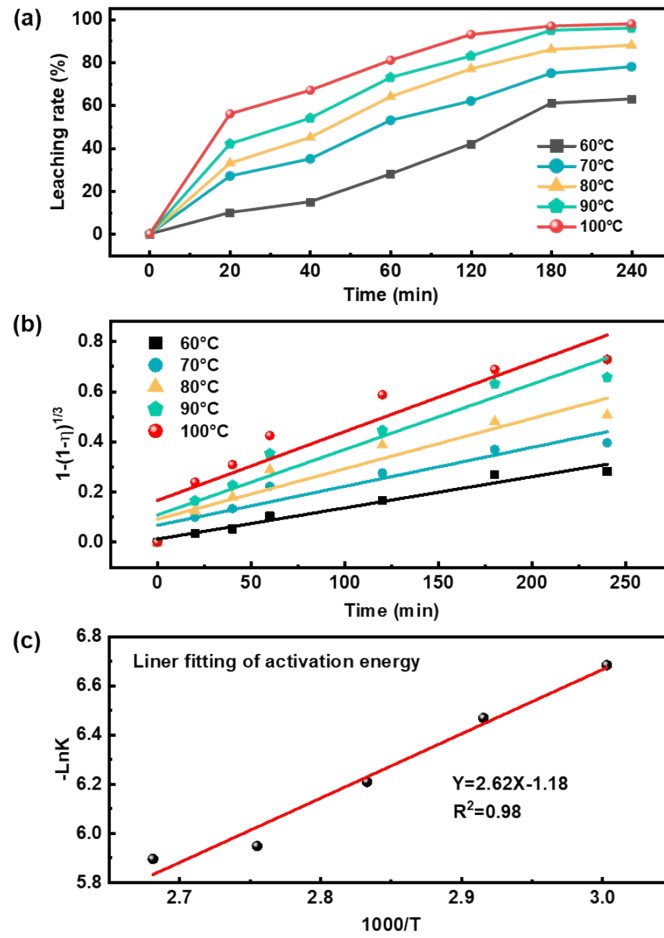


Fig. S4. (a) The leaching rate under different conditions (60-100°C, 0-240 min). (b and c) show the fitting of the activation energy ($E_a = 21.7$ kJ/mol) in the leaching process.

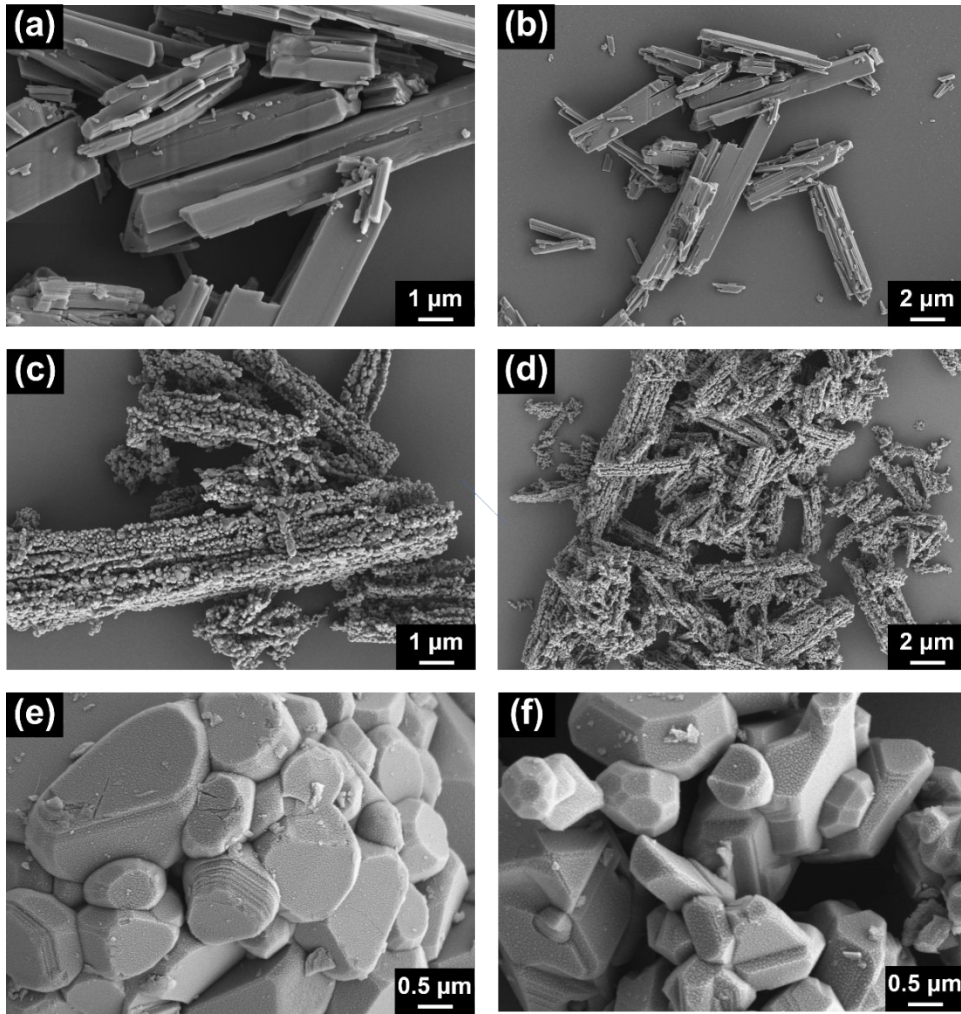


Fig. S5. SEM images of the precipitated brick-like $\text{CoC}_2\text{O}_4 \cdot 2\text{H}_2\text{O}$ phase (a and b) and the annealed Co_3O_4 (c and d). The annealed Co_3O_4 resembles the morphology of the $\text{CoC}_2\text{O}_4 \cdot 2\text{H}_2\text{O}$ precursor, while pores were formed due to the topological shrinkage of the lattice; (e) the commercial LCO and (f) the regenerated LCO.

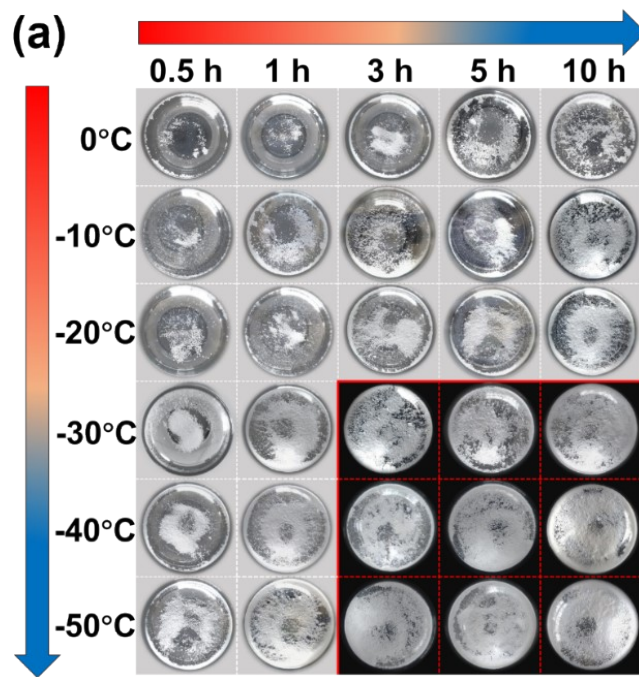


Fig. S6. 5x magnification version of digital photos.

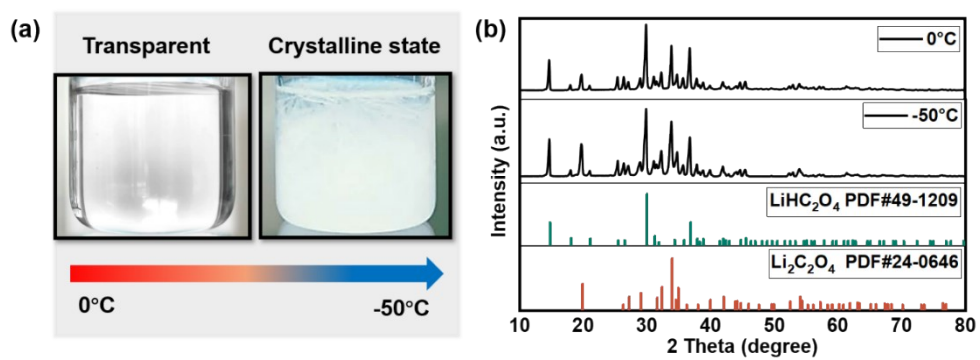


Fig. S7. (a) Digital photos visualizing the lithium element can be extracted by direct cooling. (b) XRD patterns of the precipitated lithium compound recovered at different temperatures.

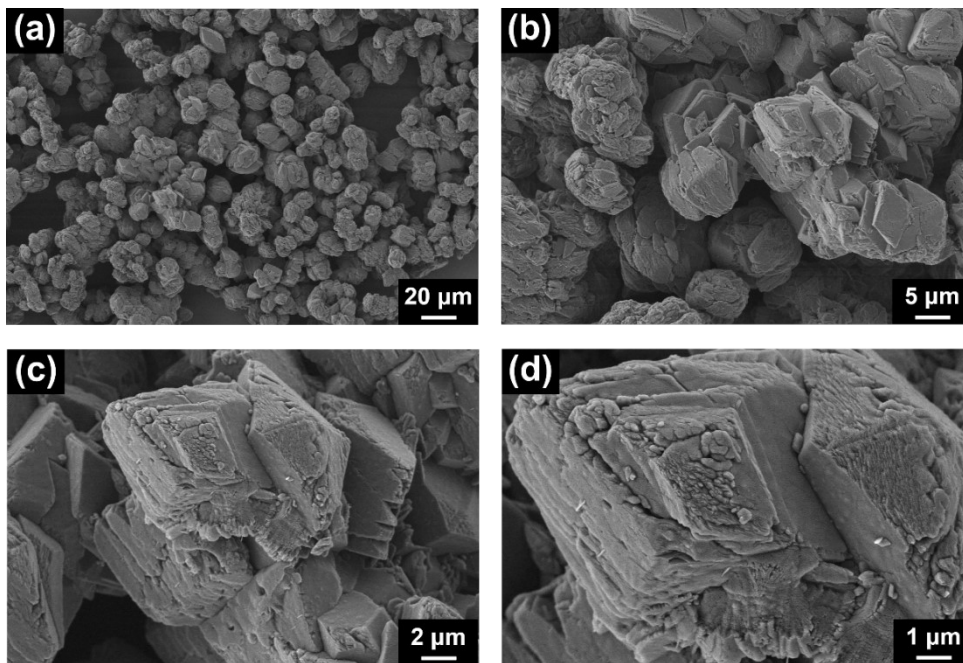


Fig. S8. SEM images of the precipitated Li compound in the form of oxalic salt.

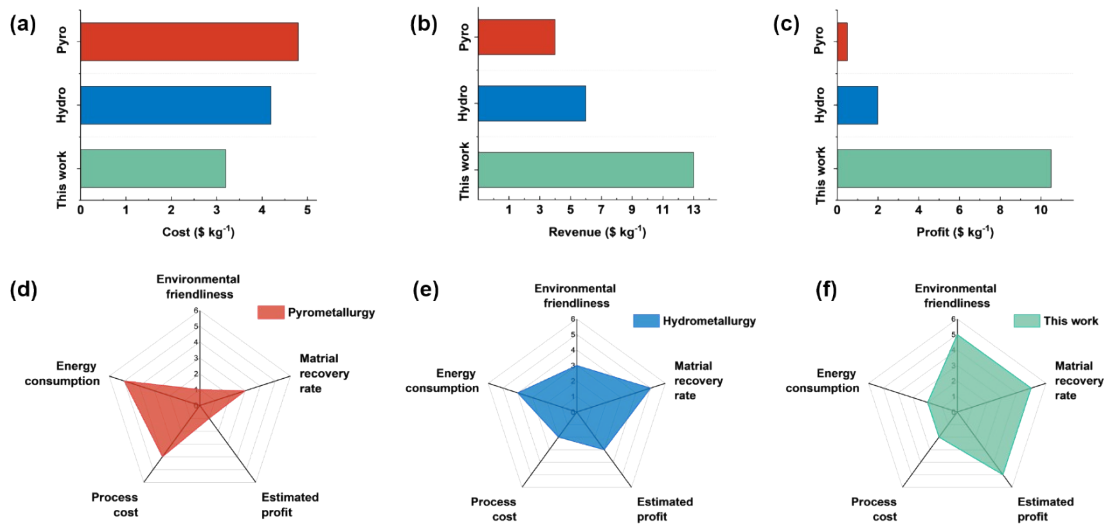


Fig. S9. Energy and economic analysis of other recycling approaches and this work. (a) Cost, (b) revenue and (c) profit for Pyrometallurgy, Hydrometallurgy and this work. Radar charts with parameters in terms of environment and economy for (d) Pyrometallurgy, (f) Hydrometallurgy and (g) this work.

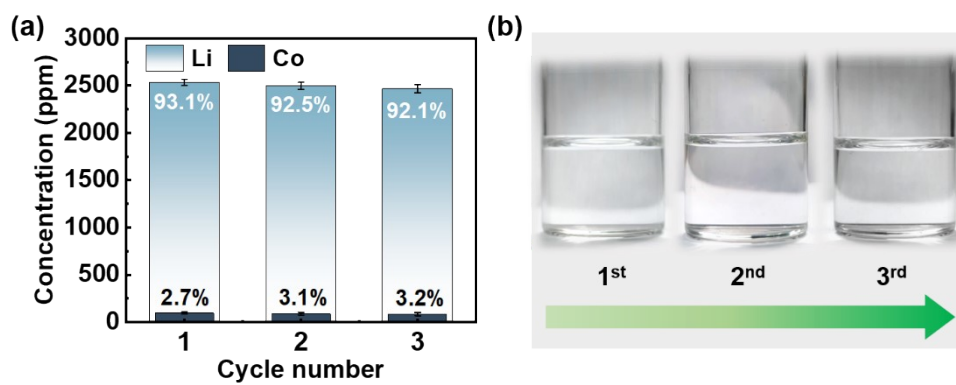


Fig. S10. Cycle performance of DES (90°C, 3 h). (a) Leaching efficiencies of Li and Co at different cycle numbers and (b) digital photos of DES after multiple cycles.

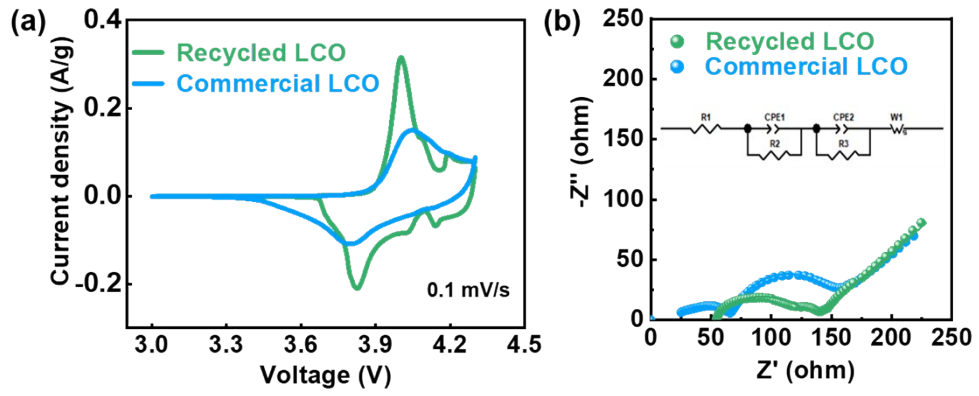


Fig. S11. (a) The CV and (b) EIS spectrum of the recycled and the commercial LCO samples.

References

1. Z. Chen, R. Feng, W. Wang, S. Tu, Y. Hu, X. Wang, R. Zhan, J. Wang, J. Zhao, S. Liu, L. Fu and Y. Sun, *Nature Communications*, 2023, **14**, 4648.
2. L. P. He, S. Y. Sun, X. F. Song and J. G. Yu, *Waste Manage.*, 2017, **64**, 171-181.
3. W. Gao, X. Zhang, X. Zheng, X. Lin, H. Cao, Y. Zhang and Z. Sun, *Environ. Sci. Technol.*, 2017, **51**, 1662-1669.
4. T. Li, Y. Xiong, X. Yan, T. Hu, S. Jing, Z. Wang and X. Ge, *J. Energy Chem.*, 2022, **72**, 532-538.
5. Y. Hua, Y. Sun, F. Yan, S. Wang, Z. Xu, B. Zhao and Z. Zhang, *Chem. Eng. J.*, 2021, **436**, 133200.
6. P. Panagiotopoulou, E. E. Karamerou and D. I. Kondarides, *Catal. Today*, 2013, **209**, 91-98.
7. A. Verma, R. Kore, D. R. Corbin and M. B. Shiflett, *Ind. Eng. Chem. Res.*, 2019, **58**, 15381-15393.
8. Q. Lu, L. Chen, X. Li, Y. Chao, J. Sun, H. Ji and W. Zhu, *ACS Sustain. Chem. Eng.*, 2021, **9**, 13851-13861.
9. J. Li, G. Wang and Z. Xu, *Journal of Hazardous Materials*, 2016, **302**, 97-104.
10. J. Lin, C. Liu, H. Cao, R. Chen, Y. Yang, L. Li and Z. Sun, *Green Chemistry*, 2019, **21**, 5904-5913.
11. Y. Tang, B. Zhang, H. Xie, X. Qu, P. Xing and H. Yin, *Journal of Power Sources*, 2020, **474**, 228596.
12. J. Wang, Z. Liang, Y. Zhao, J. Sheng, J. Ma, K. Jia, B. Li, G. Zhou and H.-M. Cheng, *Energy Storage Materials*, 2022, **45**, 768-776.
13. T. Aikawa, M. Watanabe, T. M. Aida and R. L. Smith, *Kagaku Kogaku Ronbunshu*, 2017, **43**, 313-318.
14. F. Pagnanelli, E. Moscardini, G. Granata, S. Cerbelli, L. Agosta, A. Fieramosca and L. Toro, *Journal of Industrial and Engineering Chemistry*, 2014, **20**, 3201-3207.
15. G. Nayaka, J. Manjanna, K. Pai, R. Vadavi, S. Keny and V. Tripathi, *Hydrometallurgy*, 2015, **151**, 73-77.
16. G. Nayaka, K. Pai, G. Santhosh and J. Manjanna, *Hydrometallurgy*, 2016, **161**, 54-57.
17. N. Peeters, K. Binnemans and S. Riaño, *Green Chemistry*, 2020, **22**, 4210-4221.
18. M. K. Tran, M.-T. F. Rodrigues, K. Kato, G. Babu and P. M. Ajayan, *Nature Energy*, 2019, **4**, 339-345.
19. S. Wang, Z. Zhang, Z. Lu and Z. Xu, *Green Chemistry*, 2020, **22**, 4473-4482.
20. S. Tang, M. Zhang and M. Guo, *ACS Sustainable Chemistry & Engineering*, 2022, **10**, 975-985.
21. J. R. L. Rumble, D. R.; Bruno, T. J., *CRC handbook of chemistry and physics: a ready-reference book of chemical and physical data.*, CRC Press: Boca Raton, 2018.